Identification of Carotid Plaques Composition through a Compact Microwave Sensor

Rania Shahbaz, Frédérique Deshours, Georges Alquié, Chaouki Hannachi, Hamid Kokabi, Fabien Koskas, Isabelle Brocheriou, Gilles Le Naour, Jean-Michel Davaine

Identification of Carotid Plaques Composition through a Compact Microwave Sensor

R. Shahbaz[1], F. Deshours[1], G. Alquie[1], C. Hannachi[1], H. Kokabi[1], F. Koskas[2], I. Brocheriou[3], G. Le Naour[3] et J-M. Davaine[2]
[1]*Sorbonne Université, CNRS, Laboratoire Génie Électrique et Électronique de Paris, F-75005 Paris, France*
[2]*Sorbonne Université, Service de chirurgie vasculaire, Pitié Salpêtrière, F-75013 Paris*
[3]*Sorbonne Université, Service d'Anatomie et cytologie pathologiques, Pitié Salpêtrière, F-75013 Paris*
rania.shahbaz@sorbonne-universite.fr

Abstract - Microwave biosensor brings the prominent promise of dielectric parameters detection to characterize biological tissues. This promise has already been materialized in multiple fields of healthcare and body parts. Yet when it comes to carotid plaque sticking to basic simulations, and correlating that with real-time measurements is arguably much harder. Measuring and simulating carotid plaques comprise a wide range of sub-problems, such as the heterogeneity and uniquity of each plaque, the different thicknesses, and various areas of interest. In this study, a miniaturized microwave biosensor was proposed to perform dielectric characterizations of atheromatous plaques present in arterial tissues. The designed microwave biosensor employs a Complementary Split Ring Resonator (CSRR) topology at 2.3 GHz. Electromagnetic modeling and experimental characterization have been carried out to validate the developed equivalent electrical model with very good precision and to calibrate it using other material. Atheroma measurements were achieved and compared to data obtained by simulation and then correlated with the histology results.

Keywords: Resonator, CSRR, biosensor, microwave, carotid plaque.

I. INTRODUCTION

The advancement in the medical treatment of atheromatous diseases by OMT (Optimal Medical Therapy) in the last few years has left the surgical indications for Carotid Endarterectomy (CEA) questionable and ambiguous. Atheromatous carotid stenosis causes 20 to 30% of ischemic strokes and is found in a large number of asymptomatic patients aged over 50-60 years [1]. Therefore, the development of innovative and non-invasive techniques to estimate the aggressiveness and scalability of carotid plaques and hence establish the indications for CEA is majorly needed.

Historically, CEA indication was based on studies using arteriography to evaluate the lesion. Arteriography is not able to analyze the vessel wall but only provides a degree of stenosis. This latter correlates with the risk of a cardiovascular event. However, it is widely recognized today that other parameters, in particular the composition of the plaque and its vulnerability, plays a critical role in the clinical behavior of carotid atherosclerotic plaques. The current indications are based on randomized trials in the 1990s [2, 3], which established the benefit of the intervention on so-called "symptomatic" (minor ischemic attack) and "asymptomatic" [4] stenosis whose degree of stenosis (easily measurable by echo-Doppler, angio-CT or angio-MRI) is greater than 70%. Indeed, beyond this figure, the risk of stroke is greater than the surgical risk, and the inaugural ischemic attack is usually severe in around 50% of the cases. These elements justify preventive surgery for "asymptomatic" patients. However, the benefit of surgery is questionable by recent advances in medical treatment [5]. In addition, the degree of stenosis alone does not take into account the physiological, anatomical, and hemodynamic complexity of carotid atheromatous plaque [4, 6]. It is recognized that the composition of the plaque in lipid, calcium, and or fibrous tissue, strongly influences its clinical behavior. In particular, the calcium component of an atherosclerotic plaque, both at the early and late stages of its formation, does strongly influence the stiffness of the wall, the stability of the plaque, and its risk of rupture [7, 8]. Moreover, the hemodynamic significance of carotid stenosis routinely based on diameters (NASCET) [2] is conceptually out of date as it is incongruent when compared to the overall visualization of the arterial circulation of the neck and the brain (Willis system).

The modalities currently used to preoperatively evaluate carotid plaque lesions are multi-detector CT scanner (MDCT), Doppler ultrasound and MRI. At the moment, none of these modalities is able to define the carotid plaque composition. They principally demonstrate the plaque morphology and luminal stenosis. Presently, the gold standard and the only technique to characterize the plaque composition, therefore vulnerability, is histology. Current medical research acknowledges thin fibrous cap, large necrotic core and presence of intra-plaque hemorrhage (IPH) as the best markers of vulnerable plaques [9, 10, 11].

This brings us to the core of this study, the innovative promising microwave biosensor that was developed in our GeePs laboratory. Fundamentally, the dielectric constant shift caused by placing the carotid plaque on the microwave resonator could potentially distinguish highly calcified plaques from soft

risky plaques. The goal of this study is to investigate the potential of microwave resonators and to develop it into a biosensor that would allow preoperative exploration of atherosclerotic lesions in patients.

In this study, the atheromatous biological tissue is evaluated using the microwave sensor and histological analysis. The aim is to correlate the results in order to validate the device.

II. MEDICAL METHODS

Thirty-three carotid arteries from thirty-three patients (9 females, mean age 71 ± 9 years) were included. Seven patients were symptomatic. All patients presented with a ≥ 70% carotid arterial stenosis determined by Computed tomography angiography (CTA) & ultrasound imaging (NASCET criteria) and were scheduled for carotid endarterectomy (CEA) between January and December 2020.

Exclusion criteria consisted of prior carotid artery surgery of the same side, prior carotid artery endovascular procedures or prior cervical radiation. Patients were considered symptomatic if they had experienced transient ischemic attack (TIA), amaurosis fugax (AF), central retinal artery occlusion (CRAO) or stroke ipsilateral to the carotid lesion being studied within two months prior to surgery. Silent infarcts and lacunar symptomatology, diagnosed by a neurologist based on clinical and brain computer tomography (CT) scan and/or magnetic resonance imaging (MRI) located ipsilateral to the stenosis, were also considered symptomatic.

The institutional review board at "Hôpitaux Universitaires Pitié Salpêtrière - Charles Foix" approved the study and patient consent was waived. Patient demographics, comorbidities included age, sex, race, obesity (defined as body mass index ≥ 30 kg/m2), smoking status, hypertension, diabetes mellitus, end stage renal disease (ESRD), coronary artery disease (CAD), prior coronary artery bypass graft (CABG) or percutaneous coronary intervention (PCI), atrial fibrillation (AF), lower extremity peripheral arterial disease (PAD), prior head/neck radiation, chronic obstructive pulmonary disease (COPD) and medications were recorded at the time of enrollment.

A. *Carotid Endarterectomy (CEA)*

During the surgery, carotid plaques are extracted by endarterectomy at the bifurcation from within the lumen as a single specimen. The plaque then is cut by the vascular surgeon into two identical samples longitudinally i.e. parallel to the lumen (Figure 1.a). One sample is immersed in formol after removal and sent to the histology department. The second is immersed in physiological serum and reserved in the suitable conditions until being measured by the microwave sensor. All surgical details are documented and entered in the excel sheet of the patient with the baseline data. Surgical details include: date of operation, surgical technique used (direct suture, eversion, patch or bypass), hospitalization period, post-operative stroke / TIA, date of post-operative stroke / TIA, re-intervention within 30 days of the surgery (type of re-intervention and its details), death and the results of the post-op Doppler ultrasound.

B. *Histology*

Histological analysis is performed by an experienced histopathologist (blind to the clinical details and to other modalities assessment), based on American Heart Association classification for human atherosclerotic lesions [11, 12]. For this study, the samples were fixed in 10% buffered formalin, then decalcified if necessary with a decalcification solution (surgipah Decalcifier II-Leica), and immersedin paraffin. Histological

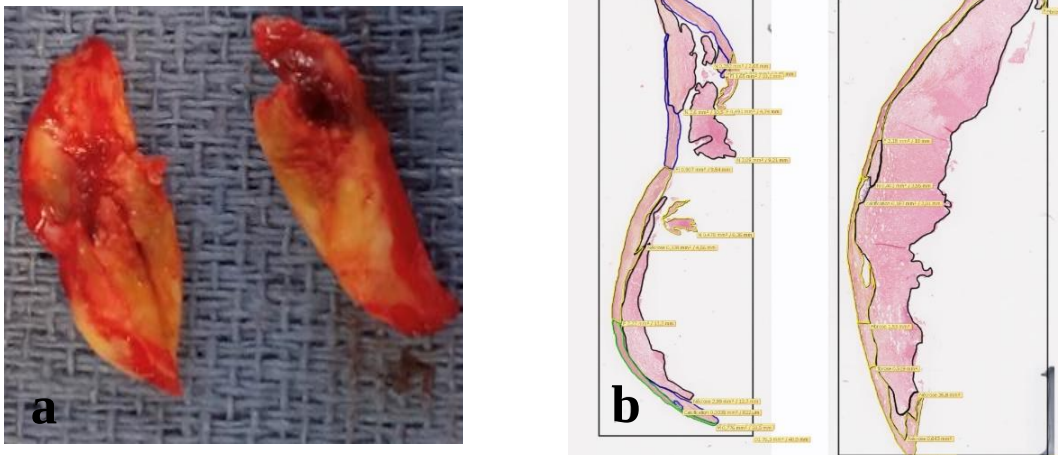

Figure 1. (a) Imaging findings in a symptomatic patient with ulcerated carotid plaque. (b) Histologic examination results, which demonstrates a plaque with fibrous intimal cap, foam cells, and cholesterol deposition.

sections with a thickness of 3 microns were prepared and stained with HES staining (Hematein, Eosin, Saffron). The total sectional area of each slide was scanned at 40X magnification with a resolution of 0.24 micron/pixel by a Nanozoomer Hamamatsu scanner. Then the digital slides were viewed on high definition screens (BARCO Coronis Fusion) in order to precisely locate the different types of tissues. All regions were manually outlined with (Viewer - NDP.view2) in order to obtain an accurate mapping and area of each component of the atherosclerotic plaque sample (Figure 1.b). This semi-quantitative analysis is performed to determine the presence of calcification (CAL), lipid-rich necrotic core (LRNC), intra-plaque hemorrhage (IPH), and fibrous cap (FC).

III. MICROWAVE BIOSENSOR DESIGN

A. *Principle of the resonance method*

Microwave resonators have specific resonance features based on their dimensions and the dielectric properties of the substrate on which they are implemented. In order to characterize biological tissues, we opted for a resonant microwave technique, which allows good sensitivity even when the materials studied exhibit high dielectric losses. Generally, the unknown dielectric material (e.g. carotid plaque) filling partially the resonator shifts the resonant frequency and broadens the curve depending on its dielectric properties. The electrical equivalent circuit of the resonator being an inductance in parallel with a capacitance, the introduction of a dielectric superstrate modifies the capacitance of this circuit. In this study, the resonator is a planar structure and the sample (called in this case "superstrate") is characterized via its application on the surface. The resonance frequency and its quality factor depend on the complex dielectric permittivity of the material, which reflects the state of its composition.

B. *Design and realization of Complementary Split Ring Resonator (CSRR)*

With the aim of performing relatively localized measurements, the unloaded resonance frequency was chosen to be around 2.4GHz (ISM frequency band), frequency retained for its relatively good penetration into the biological tissues. The resonant structure is a Complementary Split Ring Resonator (CSRR) with a circular shape engraved in the ground plane and fed by a 50 Ω microstrip line (Figure 2).

The planar resonators used are smaller than conventional resonators whose length is related to the guided wavelength λ_g at resonance; in our case, the global dimensions of the resonator is about $\lambda_g/10$. The structure consists of two interrupted concentric annular slots engraved on a FR4 dielectric substrate ε_r = 4.6; tanδ = 0.02 at 1 MHz; thickness h = 0.73mm; metallization thickness t= 35µm) (Figure 3). These CSRRs resonators are known for their relatively high quality coefficient (~ 50) when they are unloaded [14]. Our team has studied several resonator shapes thoroughly [15], and the circular one was chosen for this study. Its dimensions are optimized using HFSS software to obtain the resonance frequency around 2.4GHz. Furthermore, since biological tissues are rather moist,

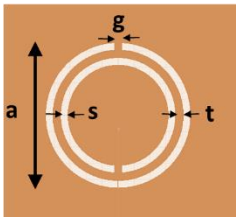

Dimensions
a= 9.08mm
g=s=t= 0.5mm

Figure 2. Geometric parameters of CSRR

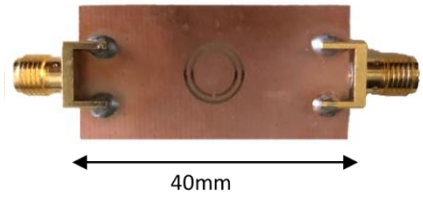

Figure 3. CSRR resonator realized on FR4 substrate

a glass plate of ε_{rv} = 7, tanδ = 0.02 and 120 µm thickness was placed on the surface of the resonator in order to avoid short-circuiting between the slits. This insulating dielectric contributes to a lowering of 140 MHz of the resonant frequency. This frequency-shift was verified using 3D full-wave electromagnetic field simulation softwares (HFSS & CST) and is taken into account in the measurements.

C. *Electrical model of CSRR*

An equivalent electrical model was developed for this resonator with and without biological samples. Since the geometric dimensions of the resonator are small compared to the wavelength, the value of the elements of the electrical equivalent schema were determined using quasi-static models for the constituent elements as well as by electrical simulations with ADS. The values of the elements of the studied resonator produced were obtained from measurements of the S parameters of the structure after de-embedding of the access lines. The equivalent RLC electric model can be extracted from it, making it possible to specify the resonant frequency (Figure 4). In the absence of a superstrate, the resonant frequency is given by relation (1):

$$f_0 = \frac{1}{2\pi\sqrt{L_R\left(C_R + C_C\right)}} \quad (1)$$

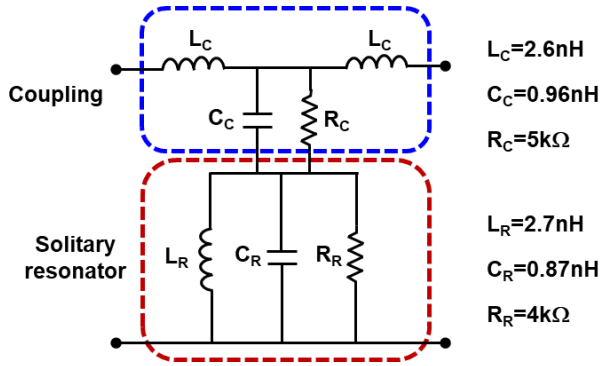

Figure 4. Equivalent electrical schema of the resonator

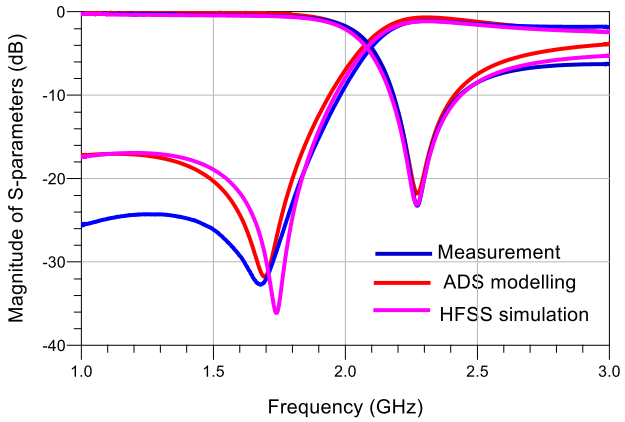

Figure 5. Graph comparing the modeling on ADS with the simulation on HFSS and the experimental measurements

The values of the elements of the resonator in its mount without a sample were extracted from characteristic frequencies measured on the S-parameters and on the Z_{11} input impedance. The principle of extraction has been proposed in reference [15].

The results of the modeling by ADS and simulations by HFSS are compared with the experimental measurements in figure 5.

D. Influence of the superstrate

By the presence of the superstrate, the capacitor C_R is increased which then lowers the resonant frequency. This frequency, denoted f_R (ε_{rs}), depends on the value of the dielectric constant ε_{rs} of this superstrate. Moreover, we can also verify that the value of $|S_{21}|$ at resonance is approximately inversely proportional to f_R^2. Electromagnetic models with HFSS made it possible to verify this dependence and to link the frequency shift with the dielectric constant of the superstrate for a material with different thicknesses. Figure 6 shows the results of HFSS & CST simulations for samples having a dielectric constant ε_{rs} between 1 and 80. Two samples thicknesses were simulated, that are 1mm and 2mm representing approximately the range of thickness of our samples.

E. Simulation results

First, the unloaded resonator (without sample) was simulated using HFSS and the resonant frequency obtained was almost exactly the same as the one measured ≈ 2.27GHz. A Plexiglas structure designed in our lab that provides the rigid support necessary to perform reproducible measurements in addition to a glass blade layer that was added to avoid short circuiting issue between the rings due to humidity of biological tissues, were simulated with the resonator and resulted in a diminution of Δ f ≈152 MHz (Figure 7).

F. Experimental setup

The sample taken by endarterectomy is analyzed within the same week of the surgical intervention. For the analysis, it is

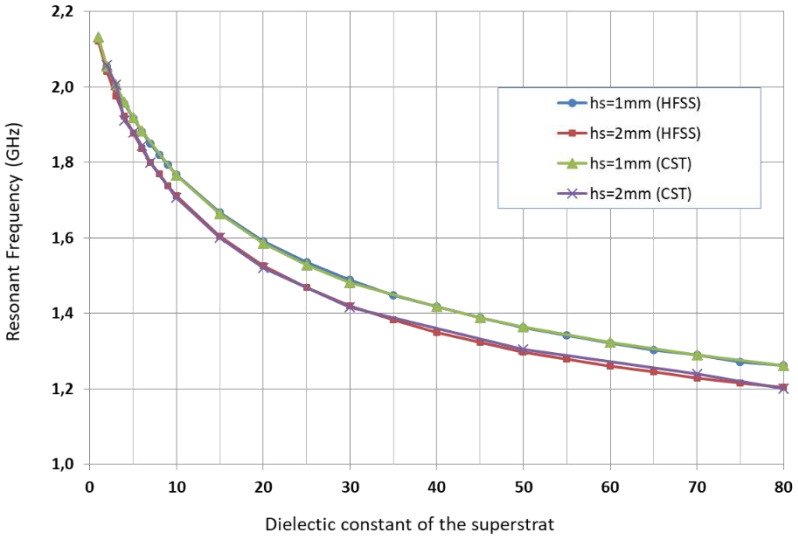

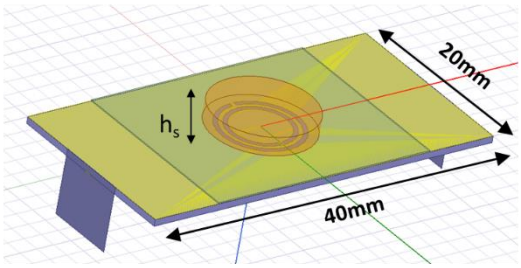

SUPERSTRAT:
h_s = 1mm ; 2mm
ε_{rs} = 1 to 10 (step 1)
ε_{rs} = 10 to 80 (step 5)
tanδ_s = 0 ; 0.1 ; 0.2 and 0.3

Figure 6. CST & HFSS simulation results of mimicking samples of biological tissues

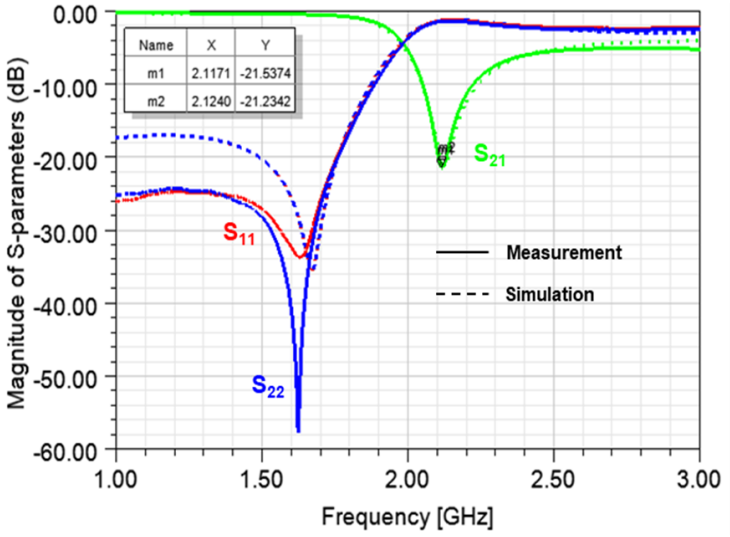

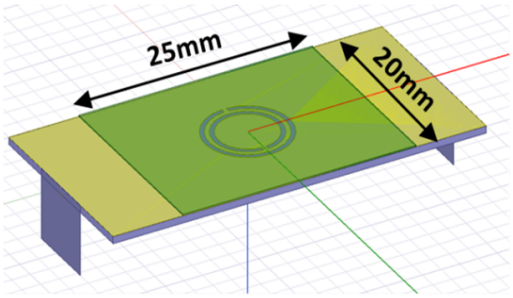

Equivalent layer of the glass blade and the plexiglass structure

Figure 7. HFSS Simulation and measurement of the resonator plus glass layer and Plexiglas

delicately dried from the physiological serum and cut in a uniform circle of 1cm diameter; at the narrowest part of the lesion, (another circular sample is cut in the case of large plaques). Plaque thickness and weight are then measured. To avoid the humidity issue, the sample is left to dry for 3 minutes, then placed on the thin layer of glass on the resonator.

The Keysight PNA-L Network Analyzer (300 kHz – 13.5 GHz) is calibrated for every set of measurements with a 3.5mm calibration kit before its connection with the resonator. Every time the testing is done, the resonator is first measured empty as a reference to ensure the matching of the baseline between measurements. The resonator is then inserted into the plexiglas structure. At that point, the round shaped atheroma plaque is inserted (Figure 8) and covered with a piston made of Teflon to eliminate air and ensure a good electrical contact with the glass cover of the resonator.

Light pressure of 300g is always applied on the piston that covers the sample to avoid the risk of deforming the plaque. The full set of scattering parameters are then recorded versus frequency and these data are exploited afterwards.

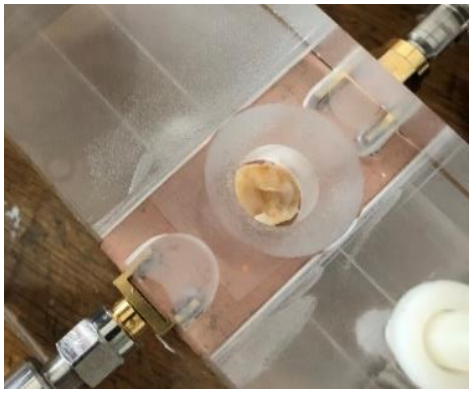

Figure 8. Sample holder setup with an atheromatous plaque

IV. Results

Thirty three samples were measured and their parameters have been extracted using HFSS. Samples had various frequency shifts and curves wideness. As expected, the dielectric constant ε_{rs} differs according to the composition of the plaque, and in a less manner with the thickness of the sample, which is partially controlled by the pressure system. This was observed by considering the frequency of the minimum of the amplitude of the transmission coefficient $|S_{21}|$ parameter which is shifted to lower frequencies as ε_{rs} increases. Results of histological analysis are not obtained until after the microwave results are produced to avoid any bias. Therefore, the samples were classified into 4 categories with the observations of the naked eye and the physical structure of the plaque. In the first 33 measured samples, it was noticed that highly calcified plaques, i.e. hard plaques, have smaller frequency shifts (≈ frequency range 1.8 GHz) and their dielectric constant is closer to that of bone ($\varepsilon_r \approx 10$). In contrast, much softer plaques (≈ frequency range 1.3 GHz) have shown higher frequency shifts and higher dielectric constant indicating the presence of a intra-plaque hemorrhage and lipid-rich necrotic core.

Figure 9 shows the results of an asymptomatic patient who had an extremely rough plaque. Upon measurements, the sample resulted in a minor shift in frequency with a 10 value for ε_{rs} while the symptomatic patient in figure 10 who developed stroke symptoms few weeks before the surgery had a high ε_{rs} and much larger shift in frequency. Their histological analysis results correlates pretty well with those finding. As in the asymptomatic

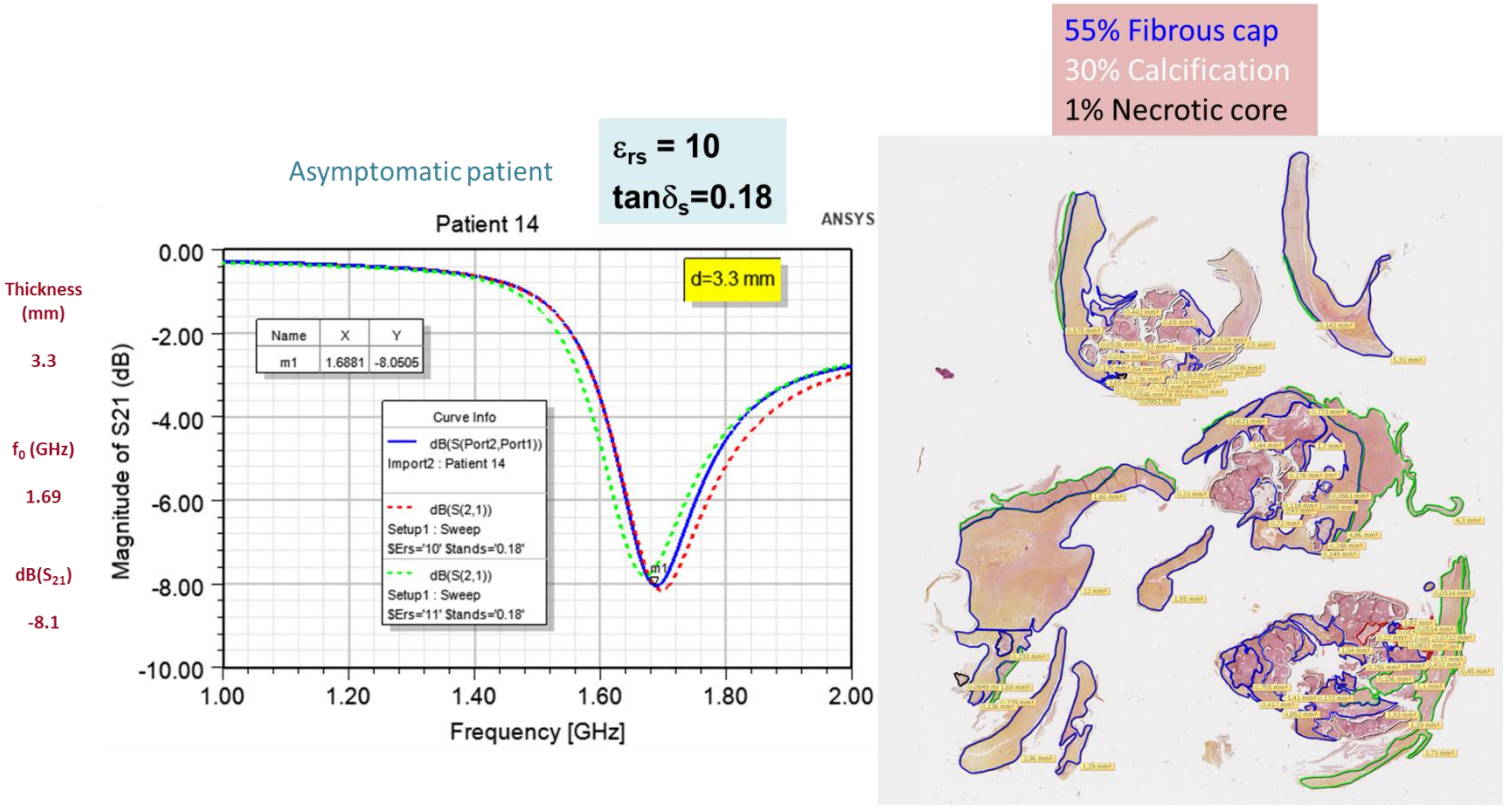

Figure 9. Constant dielectric results via HFSS and histology results of an asymptomatic patient

patient, 30% calcification was calculated in addition to 55% fibrotic tissue which are signs of stable plaque. In the contrary, the symptomatic patient had 48% lipid-rich necrotic core which is an indication for a plaque at risk. Several patients also had medial ε_{rs} like the patient in figure 11 who had 44% fibrotic tissue but also adequate amount of necrotic tissue for it to be an unstable plaque.

V. Conclusion and Perspectives

This study shows the ability of our device to analyze atheromatous carotid plaques in a standardized way. Calcified plaques displayed very different values from soft lipidic plaques. This ability to differentiate plaques according to their composition is very promising. In the first year of this research project which is in progress, 26 asymptomatic and 7 symptomatic patients have been examined. The objective is to compare at least 80 patients, 40 from each group. Based on the results achieved, a statistical correlation will be proposed between the histological parameters, the dielectric constant of the plaques and the other radiological modalities. Multivariate analysis, Bland Altman, Wilcoxson are considered as potential statistical methods. In addition, cut-off points to group plaques according to their dielectric permittivity is to be established. If the hypothesis is proved, the device is to be developed into an in-vivo portable device that could be used in hospital settings by medical staff. To achieve that, a study of multilayered samples including skin, fat and the vessel wall will be considered. Moreover, a parallel feed circular resonator is being considered for larger plaques.

Acknowledgment

We thank Mr. Yves Chatelon for his investment in the production of the Plexiglas structure, Dr. Marie-Pierre Gobin-Metteil and Dr. Josette Le Doeuff for their constant support and review of the ultrasound results and we also thank Dr. Nadjia Kachenoura and Dr. Thomas Dietenbeck for their CT scan analysis support.

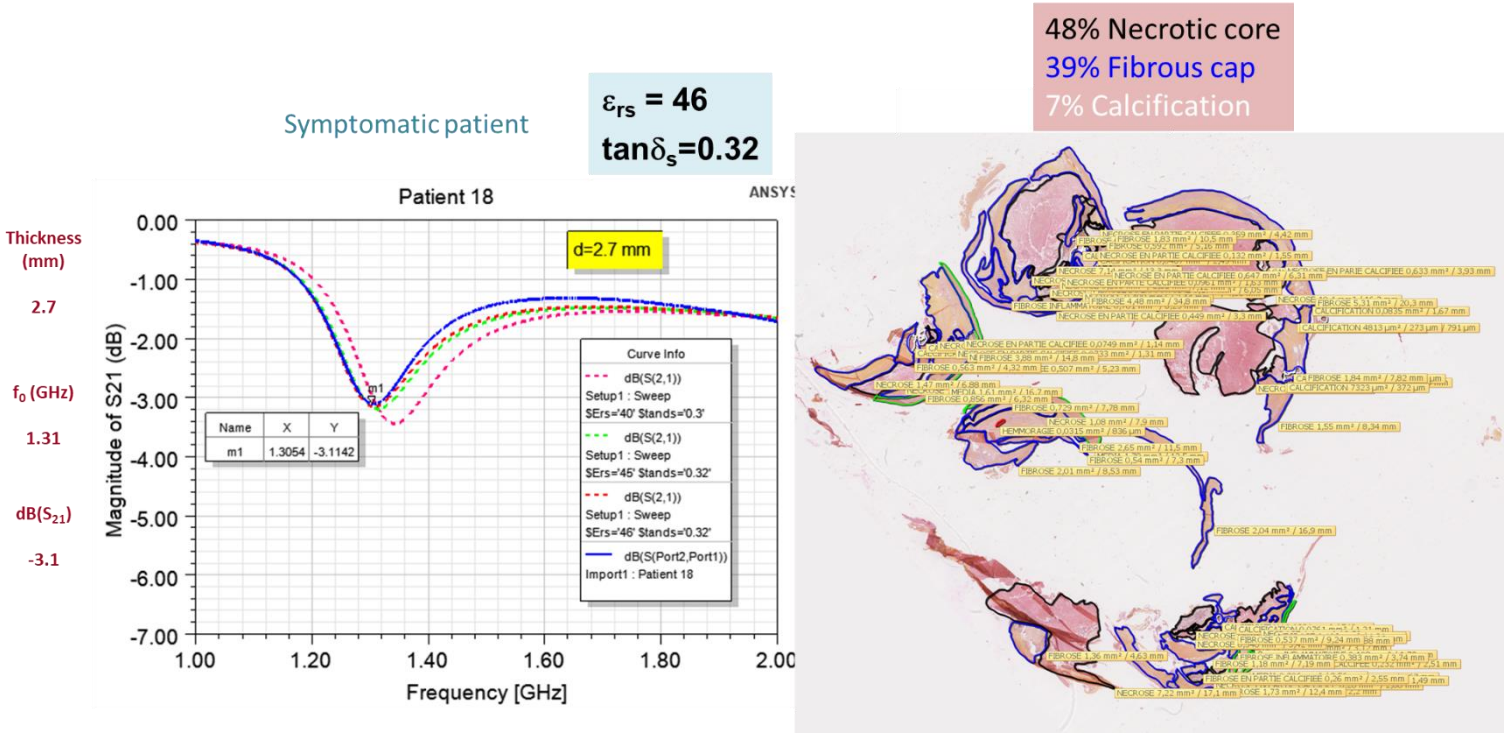

Figure 10. Constant dielectric results via HFSS and histology results of a symptomatic patient

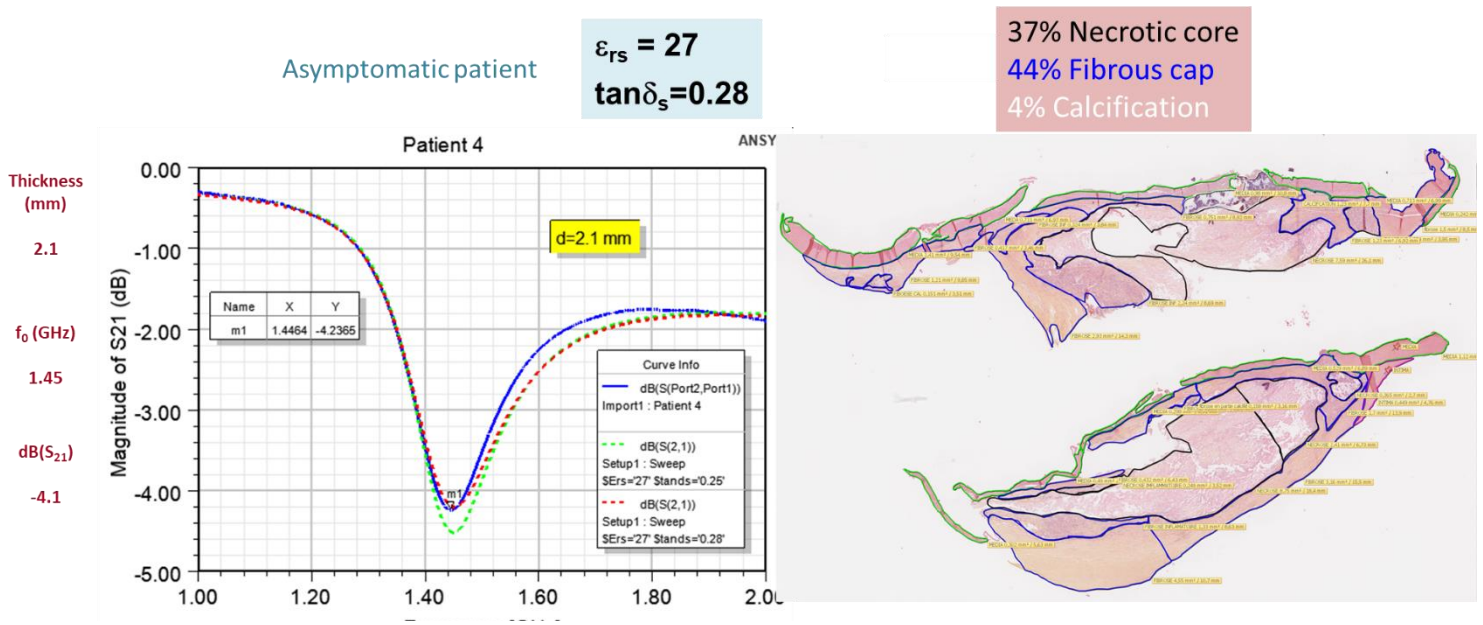

Figure 11. Constant dielectric results via HFSS and histology results of an asymptomatic patient with a risky plaque

REFERENCES

1. Santé Publique France. Accident vasculaire cérébral. 2021 [online] Available at: <https://www.santepubliquefrance.fr/maladies-et-traumatismes/maladies-cardiovasculaires-et-accident-vasculaire-cerebral/accident-vasculaire-cerebral> [Accessed December 2029].
2. North American Symptomatic Carotid Endarterectomy Trial Collaborators: H.J.M. Barnett, D.W. Taylor, R.B. Haynes, D.L. Sackett, S.J. Peerless, G.G. Ferguson, A.J. Fox, R.N. Rankin, V.C. Hachinski, D.O. Wiebers, M. Eliasziw "Beneficial effect of carotid endarterectomy in symptomatic patients with high-grade carotid stenosis", *N Engl J Med.*, vol. 325, no. 7, pp. 445-453, 1991.
3. Randomized trial of endarterectomy for recently symptomatic carotid stenosis: European Carotid Surgery Trialists' Collaborative Group "Final results of the MRC European Carotid Surgery Trial (ECST)" *The Lancet*, vol. 351(9113), pp. 1379-87, 1998.
4. ACST- Asymptomatic carotid surgery trial (ACST) collaborative group, "Prevention of disabling and fatal stroke by successful carotid endarterectomy in patients without recent neurological symptoms: randomized controlled trial". *Lancet*, vol. 363, pp. 1491-1502. 2004.
5. Brott, T. G., Halperin, J. L., Abbara, S., Bacharach, J. M., Barr, J. D., Bush, R. L., Cates, C. U., Creager, M. A., Fowler, S. B., Friday, G., Hertzberg, V. S., McIff, E. B., Moore, W. S., Panagos, P. D., Riles, T. S., Rosenwasser, R. H., Taylor, A. J., Jacobs, A. K., Smith, S. C., Yancy, C. W. ASA/ ACCF/ AHA/ AANN/ AANS/ ACR/ ASNR /CNS /SAIP/SCAI/SIR/SNIS/SVM/SVS "Guideline on the management of patients with extracranial carotid and vertebral artery disease: executive summary: a report of the American College of Cardiology Foundation/American Heart Association Task Force on Practice Guidelines, and the American Stroke Association, American Association of Neuroscience Nurses, American". *Catheterization and cardiovascular interventions: official journal of the Society for Cardiac Angiography & Interventions*. vol. 81(1). 2011.
6. Kelly-Arnold A, Maldonado N, Laudier D, Aikawa E, Cardoso L, Weinbaum S. "Revised microcalcification hypothesis for fibrous cap rupture in human coronary arteries". *Proc Natl Acad Sci U S A.* vol. 25;110 (26). pp.10741-6, 2013.
7. Davaine JM, Quillard T, Brion R, Lapérine O, Guyomarch B, Merlini T, Chatelais M, Guilbaud F, Brennan MÁ, Charrier C, Heymann D, Gouëffic Y, Heymann MF. "Osteoprotegerin, pericytes and bone-like vascular calcification are associated with carotid plaque stability". *PLoS One*. vol. 26;9 (9). pp 107-642. 2014.
8. Funaki T, Iihara K, Miyamoto S, Nagatsuka K, Hishikawa T, Ishibashi-Ueda H. "Histologic characterization of mobile and non mobile carotid plaques detected with ultrasound imaging". *J Vasc Surg*. vol. 53(4). pp. 977-83. 2011.
9. Herbert C. Stary. "Natural History and Histological Classification of Atherosclerotic Lesions". *Arteriosclerosis, Thrombosis, and Vascular Biology.* vol. 20: 5. 2000.
10. Herbert C. Stary et al., "A Definition of Advanced Types of Atherosclerotic Lesions and a Histological Classification of Atherosclerosis. A Report from the Committee on Vascular Lesions of the Council on Arteriosclerosis, American Heart Association". *Circulation and Arteriosclerosis, Thrombosis, and Vascular Biology*. vol. 92:5. 1995.
11. Saba L, Sanfilippo R, Sannia S, Anzidei M, Montisci R, Mallarini G, Suri JS. "Association between carotid artery plaque volume, composition, and ulceration: a retrospective assessment with MDCT". *AJR Am J Roentgenol*. vol. 199(1). pp.151-6. 2012.
12. M. Reiter, R. Horvat, S. Puchner, W. Rinner, P. Polterauer, J. Lammer, E. Minar, R.A Bucek "Plaque Imaging of the Internal Carotid Artery—Correlation of B-Flow Imaging with Histopathology". *AJNR Am J Neuroradiol.* vol. 28. pp.122–26. 2007.
13. Baena, J. D, Bonache, J, Martin, F, Sillero, R, M. Falcone, F. Lopetegi, T. Laso, M. A. G. Garcia-Garcia, J. Gil, I. Portillo, M. F. Sorolla, M. "Equivalent-Circuit Models for Split-Ring Resonators and Complementary Split-Ring Resonators Coupled to Planar transmissions Lines". *IEEE Transactions on Microwave Theory and Techniques*. Vol. 53, No. 4, pp. 1451-1461. 2005.
14. S. Hardinata, F. Deshours, G. Alquié, H. Kokabi and F. Koskas. "Complementary Split-Ring Resonators for Non-Invasive Characterization of Biological Tissues". *18th International Symposium on Antenna Technology and Applied Electromagnetics (ANTEM)*, Waterloo, ON, 2018, pp. 1-2. 2018.
15. F. Deshours, G. Alquié, T. Goudjil, H. Kokabi, J-M. Davaine et F. Koskas, "Modélisation de résonateurs en anneaux fendus pour la mesure de permittivités complexes", *XXIèmes Journées Nationales Microondes*, Caen, France, 14-17 mai 2019.
16. F. Deshours, G. Alquié, J-M. Davaine, L. Aboueb, A. Aissaoui, H. Kokabi. F. Koskas. T. Goudjil, O. Meyer, "Caractérisation microondes de plaques d'athérome calcifiées". *Journées d'Etude sur la TéléSanté, Sorbonne Universités*, May 2019, Paris, France.
17. Belhadj.T, Kokabi. H, Nana. S, Roduit. P, et Leprince. P. "Microwave Broad Band Measurement of Dielectric Permittivity of Normal and Calcified Human Aortic Valves". *Conference AES*, Apr 2012, Paris, France.